Extreme ultraviolet optical constants for the design and fabrication of multilayer-coated gratings

J. Seely*[a], L. Goray[b], D. Windt[c], B. Kjornrattanawanich[d], Y. Uspenskii[e], and A. Vinogradov[e]
[a]Space Science Division, Naval Research Laboratory, Washington DC 20375
[b]International Intellectual Group Inc., Box 335, Penfield NY 14526
[c]Columbia Astrophysics Laboratory, 550 West 120th Street, New York NY 10027
[d]Universities Space Research Association, National Synchrotron Light Source, Brookhaven National Laboratory, Upton NY 11973
[e]X-Ray Optics Group, Lebedev Physical Institute, 117924 Moscow, Russia

ABSTRACT

The computational design of multilayer-coated diffraction gratings for the extreme ultraviolet (EUV) wavelength region and the experimental performance of the coated gratings depend on the optical constants of the layer materials. While accurate optical constants are available for many commonly used materials, the EUV optical constants can in practice differ significantly from the tabulated values. This is generally true near absorption edges, for reactive materials that may be subject to oxidation or contamination, and for the longer EUV wavelengths (>30 nm) where molecular effects can be important. Normal-incidence gratings with Mo/Si coatings operating in the 17-21 nm and 25-29 nm wavelength ranges were successfully designed and fabricated for the Extreme Ultraviolet Imaging Spectrometer (EIS) on the Solar-B mission, the first satellite instrument to carry a multilayer grating. Examples of multilayer gratings designed and fabricated for wavelengths <12 nm and >40 nm, using materials other than Mo/Si, will be given that have in many cases required the experimental determination of the optical constants owing to inaccuracies in the tabulated values.

Keywords: Multilayer coatings, diffraction gratings, extreme ultraviolet, x-ray optics.

1. INTRODUCTION

The normal-incidence reflectances of all materials are relatively low in the EUV region, particularly for wavelengths less than approximately 30 nm. In order to achieve useful instrument sensitivity and throughput while maintaining a reasonably small collection area, multilayer interference coatings have been implemented that have high reflectance in a selected wavelength range. The computational design and fabrication of the multilayer coatings require accurate knowledge of the optical constants of the layer materials. The most commonly used EUV multilayer materials are Mo and Si and related compounds, and a number of laboratory and spaceflight telescopes and spectrometers were built for the 13-30 nm wavelength range where Si is relatively transmissive. Multilayers for wavelengths <12 nm and 30-40 nm have been developed for use on telescope mirrors, and several normal-incidence multilayer gratings with these coatings have been demonstrated. The EUV wavelength region >40 nm is largely unexplored, with the exception of Sc/Si multilayers, because of the lack of accurate optical constants for sufficiently transmissive layer materials.

A systematic study of candidate materials that may be suitably transmissive for multilayers operating at wavelengths 40-90 nm has been initiated. This study implements a novel multilayer-coated photodiode technique for measuring the optical constants of reactive materials protected by stable capping layers. Elements studied so far are Sc, Ti, La, and Tb. Several other rare earth elements are predicted to have transmission windows for wavelengths >40 nm associated with intense transitions to partially filled outer electron shells. The goal of the study is to develop high-reflectance multilayer coatings and gratings for the >40 nm wavelength region.

2. MO/SI GRATINGS FOR 13 NM - 30 NM WAVELENGTHS

Because of the excellent reliability and stability of Mo/Si multilayer coatings, they have been widely used for normal-incidence telescopes and spectrometers for laboratory and spaceflight applications. The EIS spectrometer developed for the Solar-B mission is the first satellite instrument to carry a multilayer-coated grating, and Mo/Si multilayers were selected and optimized for the instrument's mirror and grating.[1] The purpose of the spectrometer is to

Optical Constants of Materials for UV to X-Ray Wavelengths,
edited by Regina Soufli, John F. Seely, Proceedings of SPIE Vol. 5538
(SPIE, Bellingham, WA, 2004) · 0277-786X/04/$15 doi: 10.1117/12.559053

record high-resolution spectra of solar regions and to determine the properties of the emitting plasma regions from spectral line shapes, wavelengths shifts, and intensities.[2] The two halves of the grating, and the corresponding two halves of the parabolic collection mirror, are coated with Mo/Si multilayers covering the 17-21 nm and 25-29 nm wavelength ranges. The mirror has 160 mm diameter and 1.939 m focal length. The toroidal grating has 100 mm diameter, nominal 1.18 m radius of curvature, and 4200 grooves/mm with a laminar (approximately trapezoidal) groove profile.

The multilayers were deposited onto flat test mirrors, full size concave test substrates, and two pairs of flight optics at the Columbia Astrophysics Laboratory.[3] The reflectances of the flight mirror M1 at the centers of the shortband and longband sides of the mirror are shown in Fig. 1. The data points are the reflectances measured using synchrotron radiation at an angle of incidence of 2.15°,[4] and the curves are calculated reflectances. The Fresnel reflectivity and transmissivity coefficients were calculated at each material interface, and a Debye-Waller factor accounted for interdiffusion and microroughness at each interface. The layer thicknesses and interface parameters were determined by grazing incidence x-ray measurements of the test flats. Small adjustments were made to the period spacings and the interface parameters to fit the calculated normal-incidence reflectance curves to the measurements.

Shown in Fig. 1 are two calculations using the Mo and Si optical constants from the Center for X-Ray Optics (CXRO)[5] and from the National Institutes of Standards and Technology (NIST).[6] For the shortband wavelength range, the period spacing is 10.35 nm, and the ratio of the Mo to period thicknesses is 0.35. The interface parameters are 0.2 nm for the Si-on-Mo layers and 0.85 nm for the Mo-on-Si layers. For the longband range, the corresponding values are 14.65 nm, 0.34, 0.2 nm, and 0.9 nm.

There are significant differences between the calculated reflectances shown in Fig. 1, and neither calculation exactly fits the measured reflectances. The differences in the calculated reflectances primarily result from differences in the CXRO and NIST optical constants as shown in Fig. 2. While the CXRO and NIST optical constants for Si are in good agreement, except near the Si L_3 absorption edge at 12.4 nm wavelength, the CXRO and NIST optical constants for Mo significantly differ, particularly at the longer wavelengths shown in Fig. 2. This illustrates how discrepancies among published optical constants can occur even for the widely utilized Mo/Si multilayer coating.

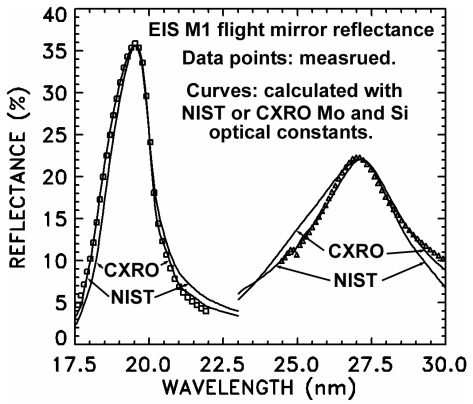

Fig. 1. The measured reflectances (data points) and the calculated reflectances (curves) of the shortband and longband EIS multilayer coatings.

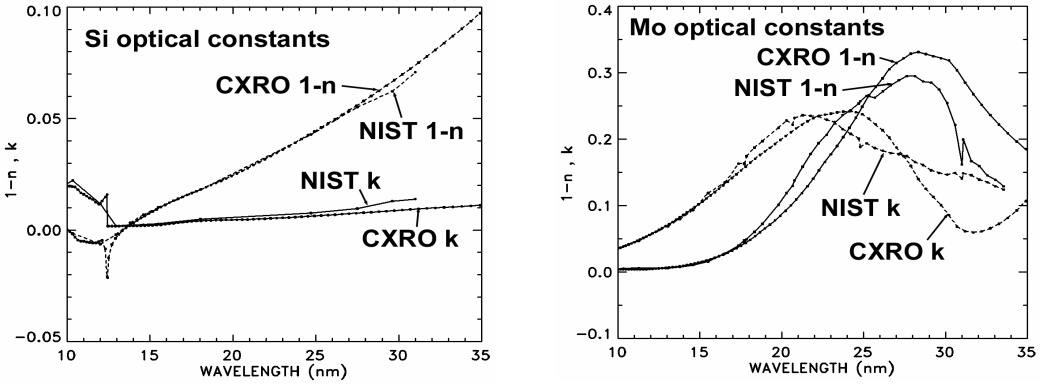

Fig. 2. The CXRO and NIST optical constants for Si (left) and Mo (right).

The same multilayer coatings were applied to both the flight gratings and flight mirrors on subsequent deposition runs. The measured and calculated efficiencies of the flight grating FL7 are shown in Figs. 3 and 4, respectively.[4] The error bars in Fig. 3 represent the standard deviation of the measurements across the coated areas of the grating.

The efficiencies were calculated using the PCGRATE computer program.[7] PCGRATE implements the modified integral method for the calculation of the efficiency of a diffraction grating with a multilayer coating. The program accounts for the optical constants of the layer materials, the two polarizations of the incident radiation, and the groove profile and microroughness as determined by atomic force microscopy (AFM). This program had been previously validated by comparison with the measured efficiencies of test gratings with gold, aluminum, and Mo/Si multilayer coatings.[1,8]

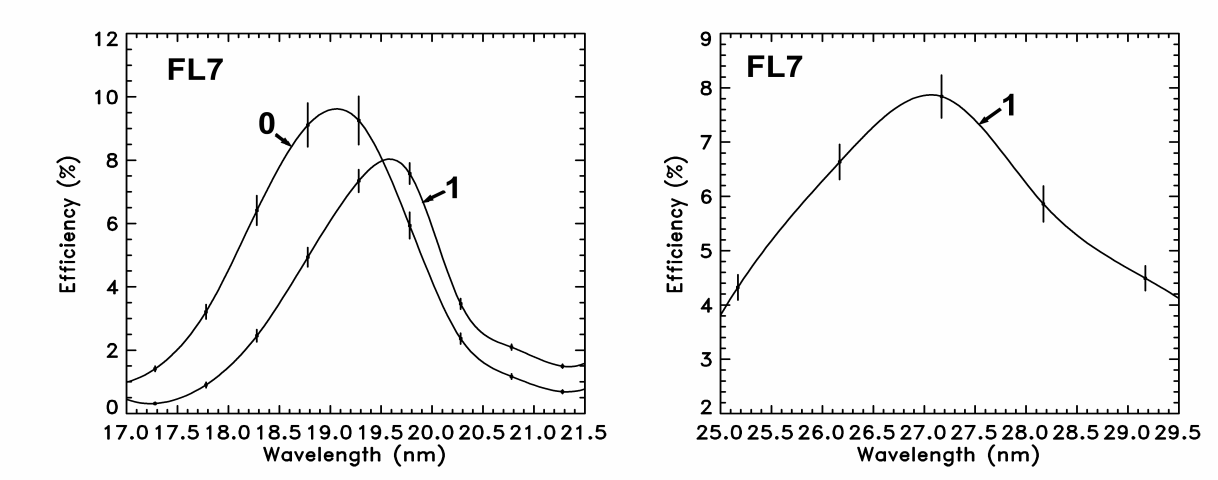

Fig. 3. The measured efficiencies of the EIS FL7 flight grating in the shortband (left) and the longband (right).

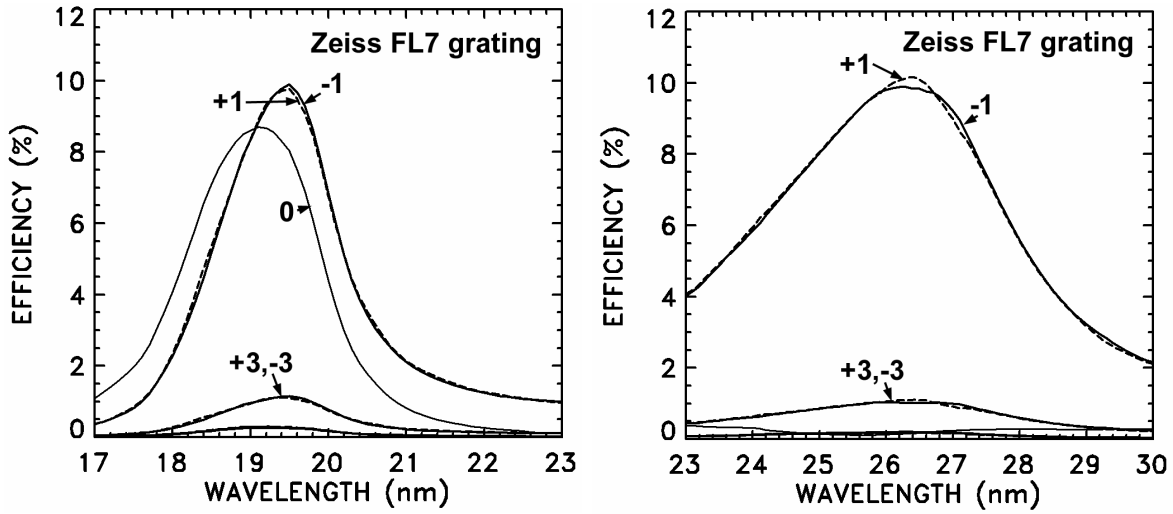

Fig. 4. The calculated efficiencies of the EIS FL7 flight grating in the shortband (left) and the longband (right).

There are significant differences between the measured and calculated efficiencies shown in Figs. 3 and 4, exceeding the differences between the measured and calculated reflectances illustrated in Fig. 1. In general for the EIS FL7 grating and for other gratings, the calculated efficiencies in the dispersed orders were larger than measured, and the calculated zero-order efficiencies were smaller than measured. These efficiency differences primarily are attributed to the uncertainties and variations in the groove profile. It was found that small changes in the groove profile used in the

PCGRATE calculation resulted in significant changes in the values of the calculated efficiencies and in the distribution of the efficiencies in the various orders.

3. MORU/BE AND MO/Y GRATINGS FOR <12 NM WAVELENGTHS

The availability of multilayer coatings with relatively high normal-incidence reflectance for wavelengths less than 12 nm, using transmissive spacer materials other than Si, has enabled the development of normal-incidence gratings in this wavelength region. MoRu/Be coatings with 50 and 100 periods were applied to two blazed grating substrates.[9,10] The grating substrates had 2400 gr/mm and were replicas of a holographic master grating with rather low microroughness (0.8 nm rms). The measured efficiencies of the master grating and a replica grating, both without a coating, were in good agreement with the PCGRATE calculations in the 10-35 nm wavelength range.[11,12]

Shown in Fig. 5(a) is the comparison of the measured (data points) and calculated (curve) reflectances of a test flat mirror with 20 MoRu/Be bilayers at an angle of incidence of 10^o. The period thickness is 6.18 nm, and the ratio of the MoRu layer thickness to the period thickness is 0.42. Based on the deposition conditions and metallurgy studies, the MoRu layers are believed to be Mo_4Ru_6. The optical constants of the Mo_4Ru_6 compound were derived from the CXRO tables for the elements Mo and Ru and assuming a density of 11.4 g/cm^3. The Be optical constants were derived from the CXRO table assuming a density of 1.85 g/cm^3. Based on experience with Be layers, the topmost Be layer was assumed to have a BeO surface of thickness 2.9 nm, and the optical constants of the BeO surface layer were derived from the Be and O CXRO data. For each interface, the Debye-Waller roughness parameter was 0.8 nm. The good agreement between the measured and calculated reflectances shown in Fig. 5(a) indicates the reliability of the optical constants derived from the CXRO tables in this wavelength region. In particular, at these short EUV wavelengths where molecular effects are rather insignificant, deriving the optical constants of compounds such as Mo_4Ru_6 and BeO from the elemental optical constants is an effective technique.

Shown in Fig. 5(b) by the data points is the measured zero-order efficiency of a replica grating with 50 MoRu/Be bilayers, and the dashed curve indicates the reflectance of the MoRu/Be multilayer on a flat mirror. The zero-order efficiency is essentially the product of the multilayer reflectance and the groove efficiency of the underlying grating substrate in the zero order. As shown in Fig. 5(b), the zero-order efficiency is a factor of 10 lower than the reflectance, and this implies that the groove efficiency of the grating substrate is 10% in the zero order. The efficiency and reflectance curves have the same oscillatory behavior, and this is related to thin-film interference effects within the multilayer coating.

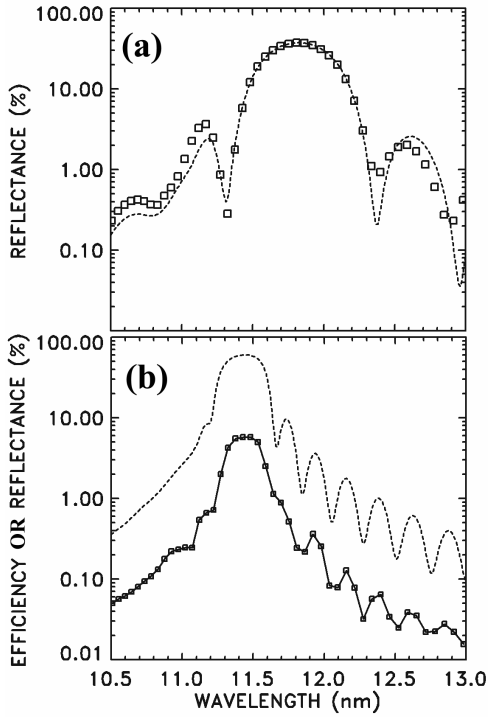

Fig. 5. (a) The measured (data points) and the calculated (dashed curve) reflectances of a test flat mirror with 20 MoRu/Be bilayers at an angle of incidence of 10^o. (b) The zero-order efficiency measured at an angle of 13.9^o (data points). Also shown is the reflectance (dashed curve) of the multilayer coating with 50 MoRu/Be bilayers. The measured zero-order efficiency is a factor of 10 lower than the reflectance.

Figure 6 is a comparison of the measured efficiencies in the diffraction orders of the MoRu/Be grating with 50 MoRu/Be periods and the efficiencies recently calculated by PCGRATE-SX version 6.1.[7] The efficiencies were calculated using the same multilayer parameters and optical constants as for the test multilayer coatings on flat mirrors. The groove profile and microroughness were derived from AFM studies of the uncoated and coated gratings. There were no free parameters in the calculation.

As seen in Fig. 6, the calculated efficiencies tend to be larger than the measured efficiencies. This may result from an incomplete understanding of the role of microroughness at these shorter EUV wavelengths. In addition, the measured inside (n<0) and outside (n>0) orders are separated in wavelength in good agreement with the efficiencies calculated using the PCGRATE-SX version 6.1 resonance calculational mode. When the PCGRATE-SX normal calculational mode is used, the computations execute much faster owing to the implementation of approximate algorithms, but the inside and outside orders are not separated in wavelength in disagreement with the measurements.

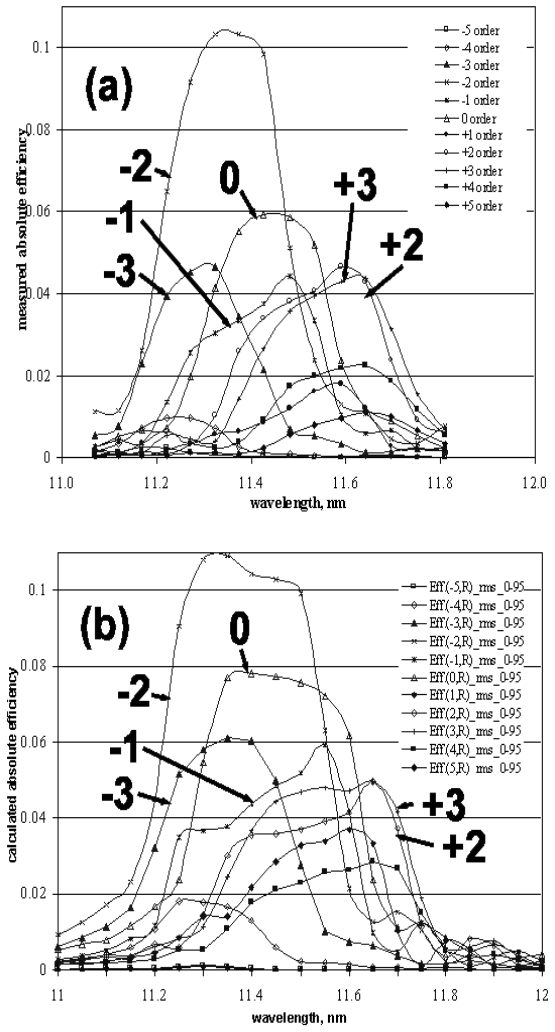

Fig. 6. (a) The efficiencies of grating #2 with 50 MoRu/Be periods measured at an angle of incidence of 13.9° and (b) The calculated efficiencies.

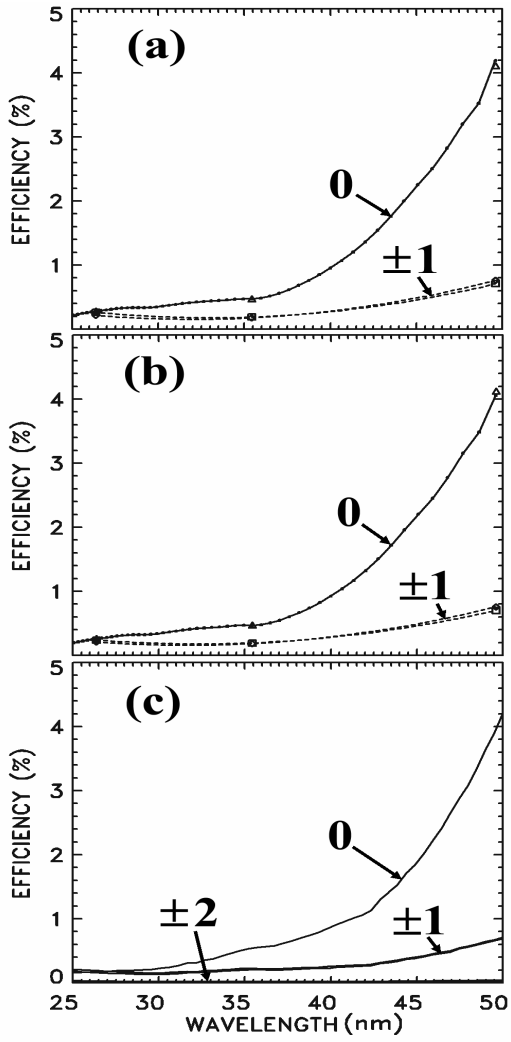

Fig. 7. The efficiencies of (a) grating #1 and (b) grating #2 measured at an angle of incidence of 13.9° and (c) The calculated efficiencies.

Figure 7 is a comparison of the measured and calculated efficiencies in the 25-50 nm wavelength range. At these longer EUV wavelengths, the reflectance is primarily from the topmost layers of the MoRu/Be coating and is characteristic of the optical constants of the topmost Be and MoRu layers. As for the shorter wavelengths, the optical constants of the BeO surface layer and the underlying Be and Mo_4Ru_6 layers were derived from the optical constants of elemental Be, O, Mo, and Ru. The layer thickness, interface, and groove parameters were the same as for the shorter wavelength calculations. Initial calculations in the 25-40 nm wavelength range using optical constants derived from the CXRO tables indicated poor agreement with the measured efficiencies. Other calculations using optical constants derived from Palik's compilation (Be,[13] Ru,[14] and Mo[15]) indicated good agreement in the 25-50 nm wavelength range as shown in Fig. 7(c). These results imply that for wavelengths >25 nm, optical constants derived from Palik's compilation may in some cases be more accurate than the CXRO values. Shown in Fig. 8 is a comparison of the optical constants of Be and Ru from CXRO[5] and Palik's compilation.[13,14] While the optical constants agree at wavelengths <20 nm, there are obvious differences for wavelengths >30 nm.

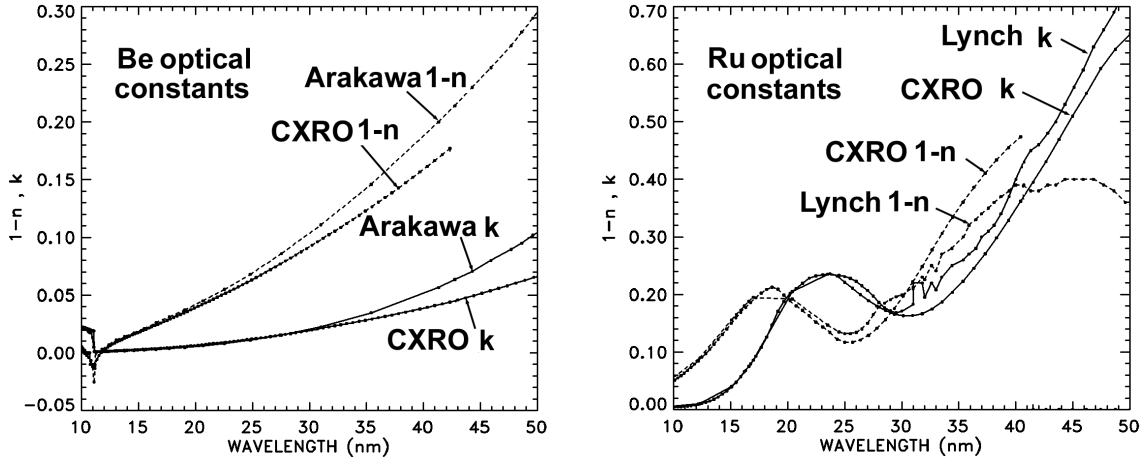

Fig. 8. The optical constants of Be and Ru derived from the CXRO tables and from Palik's compilation (Refs. 13 and 14).

Multilayers in the 7 nm to 9 nm wavelength range have been developed using yttrium as the transmissive spacer layer.[16] An Mo/Y multilayer coating was applied to a replica grating of the same type as used for the MoRu/Be grating studies.[17] The zero-order efficiency, measured at an incidence angle of 8°, is shown in Fig. 9 and is compared to the reflectance of the Mo/Y coating on a flat mirror. The ratio of the two curves shown in Fig. 9 implies a 2.8% zero-order groove efficiency. The zero-order groove efficiency (2.8%) in the 9 nm wavelength region is smaller than the corresponding groove efficiency (10%) near 11 nm, derived from the MoRu/Be grating studies, primarily because of the increasing effect of microroughness at shorter wavelengths. New values for the optical constants of Y were derived.[18]

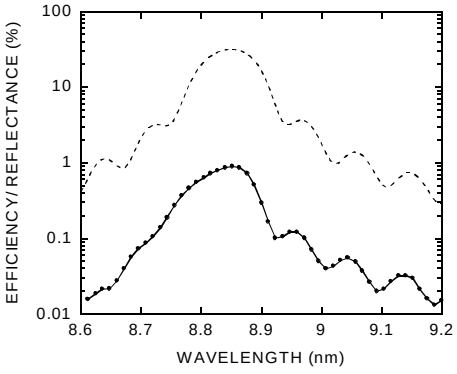

Fig. 9. The zero-order grating efficiency measured at 8° from normal incidence (lower dotted curve) and the reflectance (upper dashed curve) of the witness Mo/Y multilayer coating.

The measured and calculated efficiencies for the Mo/Y grating are compared in Fig. 10. As for the MoRu/Be grating, the calculated efficiencies tend to be larger than the measured efficiencies. In addition, the measured inside and outside orders of the Mo/Y grating are slightly shifted in wavelength as was the case for the MoRu/Be grating. The calculated efficiencies shown in Fig. 10 were computed using the PCGRATE normal calculational mode which executes much faster than the resonance calculational mode but implements approximate algorithms that result in no wavelength shift of the inside and outside orders.

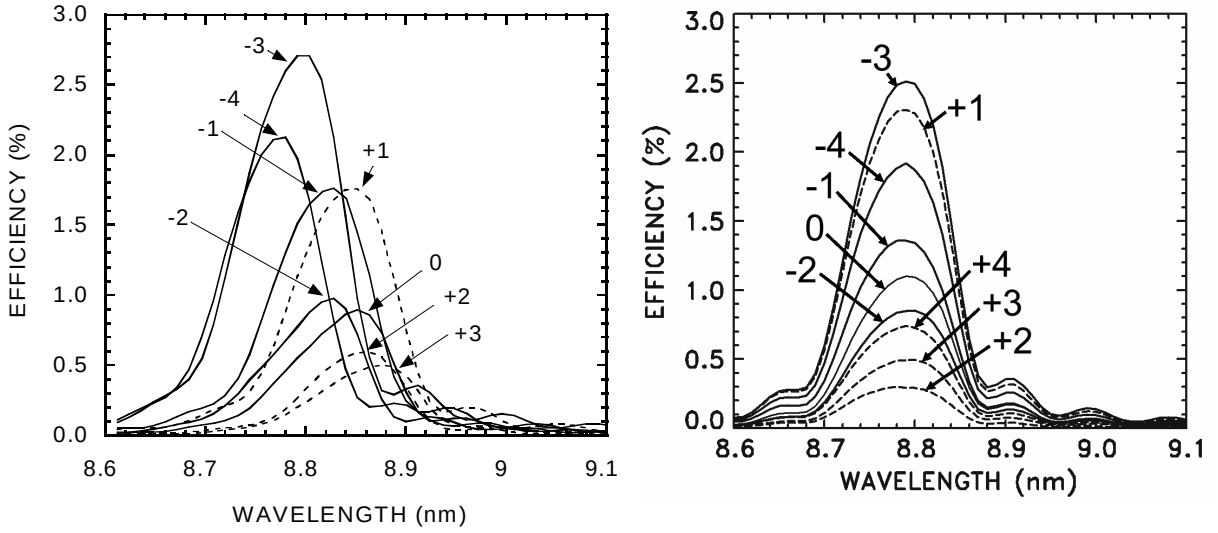

Fig. 10. Left: The efficiencies of the Mo/Y grating measured at 8° angle of incidence as a function of wavelength. The highest measured efficiency was 2.7% in the -3 order at a wavelength of 8.79 nm. Right: The grating efficiencies calculated for 8° angle of incidence as a function of wavelength.

4. SC/SI GRATINGS FOR 40-50 NM WAVELENGTHS

Multilayer coatings using Sc and Si were developed for the 40 nm to 50 nm wavelength range, primarily motivated by the need for high-reflectance coatings for a fast-discharge laser operating at a wavelength of 46.9 nm.[19] Scandium has relatively high transmittance in the 40-50 nm wavelength range because of intense transitions of the 3p core electrons to the partially filled 3d levels. The normal-incidence reflectances, measured using a laser-produced plasma radiation source, were in the range 31% to 54%.[19] Based on these results, Sc/Si multilayer coatings were deposited onto a 3600 gr/mm blazed grating substrate and at the same time onto flat witness mirrors. The coatings were designed to have peak reflectance near a wavelength of 40 nm. The reflectances of the test coatings, measured using synchrotron radiation, were unexpectedly low, typically about 25% at 40 nm wavelength.[20]

In order to understand the rather low Sc/Si multilayer reflectances measured at 40 nm wavelength, the optical constants of Sc were measured using a novel technique.[20] Scandium layers with thicknesses in the range 7.5 nm to 130 nm were deposited onto the surfaces of six silicon photodiodes. The Sc layers were protected from oxidation by Si layers of thickness 5 nm. Since each diode had the same 5 nm Si protective layer, the effect of the Si layers essentially divided out in the data analysis.[21] The attenuation coefficient k was determined from the measure transmittances of the Sc/Si bilayers, and the real part of the index of refraction was determined by the Kramers-Kronig relationship and by the measured reflectances of the Sc/Si bilayers and of Sc/Si multilayer coatings. The resulting Sc optical constants are shown in Fig. 11 along with the optical constants of Ti and La determined by the same technique. For comparison, the optical constants derived from the CXRO tables are also shown in Fig. 11. These newly determined optical constants and the CXRO values agree for wavelengths <20 nm and differ significantly for longer wavelengths. In the case of Sc, the newly determined attenuation coefficient at 40 nm wavelength is much higher than the CXRO value, and this explains the unexpectedly low Sc/Si multilayer reflectance measured at 40 nm.

Elevated temperature studies of Sc/Si multilayers indicated that the stability can be improved by using a thin tungsten barrier layer between the Sc and Si layers.[22] The comparison of the reflectance of a Sc/W/Si multilayer, measured using synchrotron radiation, and the reflectance calculated using the newly determined Sc optical constants is shown in Fig. 12. The W barrier layers were 0.8 nm thick, and the W and Si optical constants were from Palik's compilation.[23] The measured and calculated efficiencies of the Sc/W/Si coated grating are also shown in Fig. 12. The measured and calculated reflectances and efficiencies are in good agreement.

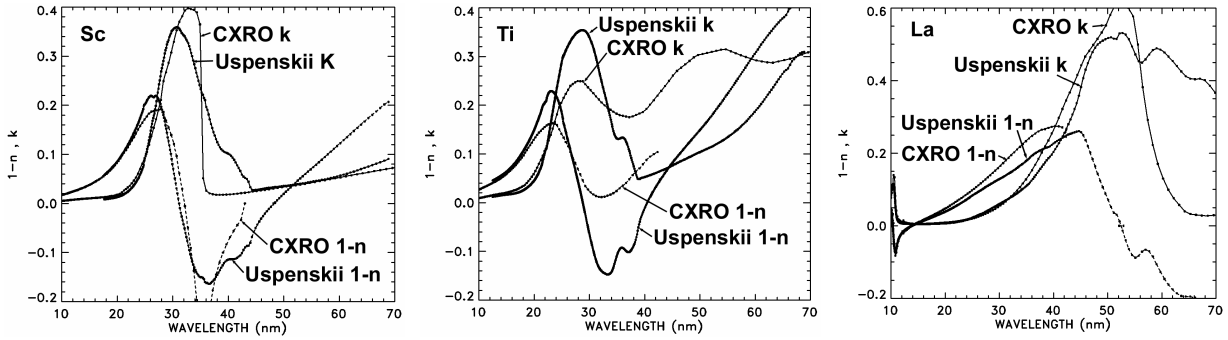

Fig. 11. The optical constants of Sc, Ti, and La derived from the transmittances and reflectances of protected bilayers of various thicknesses on silicon photodiodes by Uspenskii *et al.* are compared to the values derived from the CXRO tables.

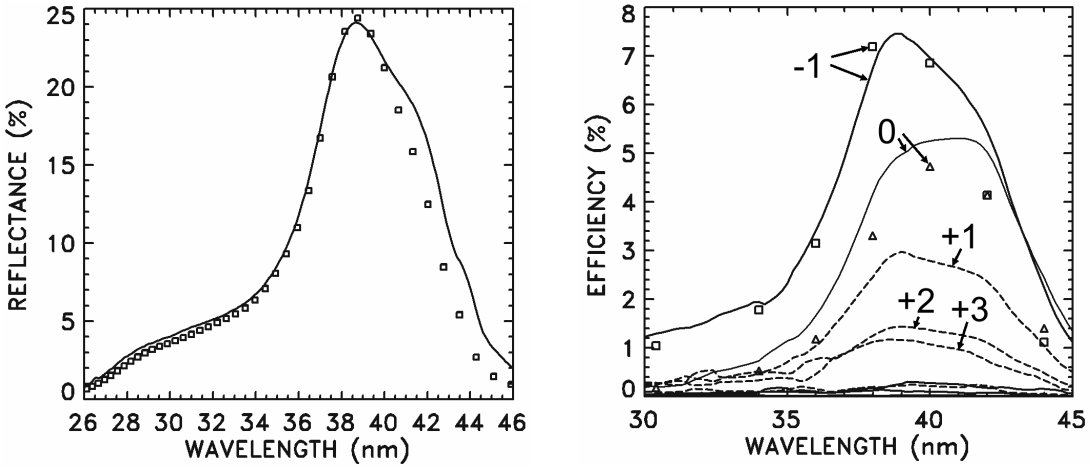

Fig. 12. Left: The measured (data points) and calculated reflectance of a Sc/W/Si multilayer test flat mirror. Right: The measured efficiencies (data points) of the Sc/W/Si grating in the -1 and 0 orders for an angle of incidence of 6°, and the calculated efficiencies (curves).

5. WAVELENGTHS >50 NM

High-reflectance multilayer coatings are required for the solar missions operating at wavelengths >50 nm. For example, imaging and spectroscopy of the intense O V spectral line at 63.0 nm has been the goal of several proposed missions. A single opaque layer of SiC has approximately 20% reflectance at 63 nm and has been used for solar instruments. A single layer of B_4C has slightly higher reflectance. An optimized $Al/MgF_2/B_4C$ coating has 29% reflectance at 63 nm.[24] A multilayer interference coating using more transmissive materials could potentially have a higher peak reflectance and also a narrower reflectance profile which is important for narrowband imaging of spectral lines such as the O V line at 63.0 nm. Thus the availability of transmissive layer materials for multilayer coatings could

potentially enhance the performance of solar instruments. However, such highly-reflective multilayer coatings are not presently available because of the lack of knowledge of the optical constants of suitably transmissive materials for wavelengths >50 nm.

Potential candidate elements for multilayers operating at >50 nm wavelengths can be identified based on the electronic structure of the elements. Looking at the portions of the periodic table of the elements shown in Fig. 13, it can be seen that the transition metals Sc and Ti are relatively transmissive in the 40-50 nm wavelength region because of intense transitions from the 3p level to the partially filled 3d level. Similarly, Sn and In are widely used transmissive filter materials because of transitions to the partially filled 5p level. The rare earth (lanthanide) elements also have partially filled outer levels (5d and 4f), and initial studies have indicated that these elements may have transmission windows at EUV wavelengths >50 nm.[25]

The partially filled outer levels make these elements reactive, and oxidation and contamination must be avoided when attempting to determine the optical constants. When utilized in multilayer coatings, the reactivity is somewhat mitigated by the alternating layer material and a protective capping layer. Thus highly-reflective multilayers using Sc, Y, and La have been fabricated and successfully utilized at <10 nm wavelengths (for example Ref. 17), and as discussed in the previous section Sc/Si multilayers have been utilized for the 46.9 nm discharge laser studies.[19]

21 $^2D_{3/2}$ **Sc** Scandium 44.95591 $[Ar]3d4s^2$ 6.5615	22 $^3F_2$ **Ti** Titanium 47.867 $[Ar]3d^2 4s^2$ 6.8281	23 $^4F_{3/2}$ **V** Vanadium 50.9415 $[Ar]3d^3 4s^2$ 6.7462	24 $^7S_3$ **Cr** Chromium 51.9961 $[Ar]3d^5 4s$ 6.7665	25 $^6S_{5/2}$ **Mn** Manganese 54.93805 $[Ar]3d^5 4s^2$ 7.4340	26 $^5D_4$ **Fe** Iron 55.845 $[Ar]3d^6 4s^2$ 7.9024	27 $^4F_{9/2}$ **Co** Cobalt 58.93320 $[Ar]3d^7 4s^2$ 7.8810	28 $^3F_4$ **Ni** Nickel 58.6934 $[Ar]3d^8 4s^2$ 7.6398	29 $^2S_{1/2}$ **Cu** Copper 63.546 $[Ar]3d^{10} 4s$ 7.7264	30 $^1S_0$ **Zn** Zinc 65.39 $[Ar]3d^{10} 4s^2$ 9.3942	31 $^2P°_{1/2}$ **Ga** Gallium 69.723 $[Ar]3d^{10} 4s^2 4p$ 5.9993	32 $^3P_0$ **Ge** Germanium 72.61 $[Ar]3d^{10} 4s^2 4p^2$ 7.8994	33 $^4S°_{3/2}$ **As** Arsenic 74.92160 $[Ar]3d^{10} 4s^2 4p^3$ 9.7886	34 $^3P_2$ **Se** Selenium 78.96 $[Ar]3d^{10} 4s^2 4p^4$ 9.7524	35 $^2P°_{3/2}$ **Br** Bromine 79.904 $[Ar]3d^{10} 4s^2 4p^5$ 11.8138
39 $^2D_{3/2}$ **Y** Yttrium 88.90585 $[Kr]4d5s^2$ 6.2173	40 $^3F_2$ **Zr** Zirconium 91.224 $[Kr]4d^2 5s^2$ 6.6339	41 $^6D_{1/2}$ **Nb** Niobium 92.90638 $[Kr]4d^4 5s$ 6.7589	42 $^7S_3$ **Mo** Molybdenum 95.94 $[Kr]4d^5 5s$ 7.0924	43 $^6S_{5/2}$ **Tc** Technetium (98) $[Kr]4d^5 5s^2$ 7.28	44 $^5F_5$ **Ru** Ruthenium 101.07 $[Kr]4d^7 5s$ 7.3605	45 $^4F_{9/2}$ **Rh** Rhodium 102.90550 $[Kr]4d^8 5s$ 7.4589	46 $^1S_0$ **Pd** Palladium 106.42 $[Kr]4d^{10}$ 8.3369	47 $^2S_{1/2}$ **Ag** Silver 107.8682 $[Kr]4d^{10} 5s$ 7.5762	48 $^1S_0$ **Cd** Cadmium 112.411 $[Kr]4d^{10} 5s^2$ 8.9938	49 $^2P°_{1/2}$ **In** Indium 114.818 $[Kr]4d^{10} 5s^2 5p$ 5.7864	50 $^3P_0$ **Sn** Tin 118.710 $[Kr]4d^{10} 5s^2 5p^2$ 7.3439	51 $^4S°_{3/2}$ **Sb** Antimony 121.760 $[Kr]4d^{10} 5s^2 5p^3$ 8.6084	52 $^3P_2$ **Te** Tellurium 127.60 $[Kr]4d^{10} 5s^2 5p^4$ 9.0096	53 $^2P°_{3/2}$ **I** Iodine 126.90447 $[Kr]4d^{10} 5s^2 5p^5$ 10.4513
57 $^2D_{3/2}$ **La** Lanthanum 138.9055 $[Xe]5d6s^2$ 5.5769	58 $^1G°_4$ **Ce** Cerium 140.116 $[Xe]4f5d6s^2$ 5.5387	59 $^4I°_{9/2}$ **Pr** Praseodymium 140.90765 $[Xe]4f^3 6s^2$ 5.473	60 $^5I_4$ **Nd** Neodymium 144.24 $[Xe]4f^4 6s^2$ 5.5250	61 $^6H°_{5/2}$ **Pm** Promethium (145) $[Xe]4f^5 6s^2$ 5.582	62 $^7F_0$ **Sm** Samarium 150.36 $[Xe]4f^6 6s^2$ 5.6437	63 $^8S°_{7/2}$ **Eu** Europium 151.964 $[Xe]4f^7 6s^2$ 5.6704	64 $^9D°_2$ **Gd** Gadolinium 157.25 $[Xe]4f^7 5d6s^2$ 6.1498	65 $^6H°_{15/2}$ **Tb** Terbium 158.92534 $[Xe]4f^9 6s^2$ 5.8638	66 $^5I_8$ **Dy** Dysprosium 162.50 $[Xe]4f^{10} 6s^2$ 5.9389	67 $^4I°_{15/2}$ **Ho** Holmium 164.93032 $[Xe]4f^{11} 6s^2$ 6.0215	68 $^3H_6$ **Er** Erbium 167.26 $[Xe]4f^{12} 6s^2$ 6.1077	69 $^2F°_{7/2}$ **Tm** Thulium 168.93421 $[Xe]4f^{13} 6s^2$ 6.1843	70 $^1S_0$ **Yb** Ytterbium 173.04 $[Xe]4f^{14} 6s^2$ 6.2542	71 $^2D_{3/2}$ **Lu** Lutetium 174.967 $[Xe]4f^{14} 5d6s^2$ 5.4259
89 $^2D_{3/2}$ **Ac** Actinium (227) $[Rn]6d7s^2$ 5.17	90 $^3F_2$ **Th** Thorium 232.0381 $[Rn]6d^2 7s^2$ 6.3067	91 $^4K_{11/2}$ **Pa** Protactinium 231.03588 $[Rn]5f^2 6d7s^2$ 5.89	92 $^5L°_6$ **U** Uranium 238.0289 $[Rn]5f^3 6d7s^2$ 6.1941	93 $^6L_{11/2}$ **Np** Neptunium (237) $[Rn]5f^4 6d7s^2$ 6.2657	94 $^7F_0$ **Pu** Plutonium (244) $[Rn]5f^6 7s^2$ 6.0262	95 $^8S°_{7/2}$ **Am** Americium (243) $[Rn]5f^7 7s^2$ 5.9738	96 $^9D°_2$ **Cm** Curium (247) $[Rn]5f^7 6d7s^2$ 5.9915	97 $^6H°_{15/2}$ **Bk** Berkelium (247) $[Rn]5f^9 7s^2$ 6.1979	98 $^5I_8$ **Cf** Californium (251) $[Rn]5f^{10} 7s^2$ 6.2817	99 $^4I°_{15/2}$ **Es** Einsteinium (252) $[Rn]5f^{11} 7s^2$ 6.42	100 $^3H_6$ **Fm** Fermium (257) $[Rn]5f^{12} 7s^2$ 6.50	101 $^2F°_{7/2}$ **Md** Mendelevium (258) $[Rn]5f^{13} 7s^2$ 6.58	102 $^1S_0$ **No** Nobelium (259) $[Rn]5f^{14} 7s^2$ 6.65	103 $^2P°_{1/2}$? **Lr** Lawrencium (262) $[Rn]5f^{14} 7s^2 7p$? 4.9 ?

Fig. 13. Portions of the periodic table of the elements.

Based on the technique discussed in the previous section for determining the optical constants of reactive materials, by depositing protected layers on silicon photodiode substrates, a systematic study of the optical constants of the rare earth elements is in progress. The optical constants of La are shown in Fig. 11. Based on the CXRO tables, La was predicted to have good transmittance at 63.0 nm wavelength. However, as seen in Fig. 11, the measured La attenuation coefficient k is much larger than predicted by the CXRO tables.

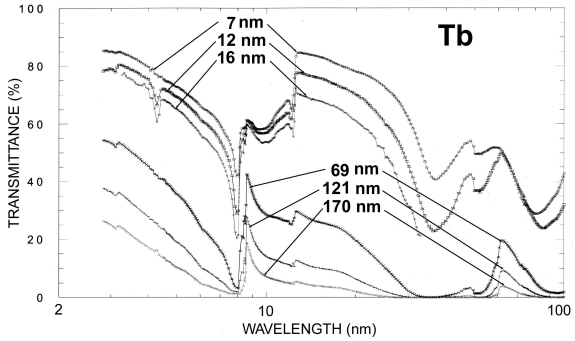

Fig. 14. The measured transmittances of Tb/Si bilayers on silicon photodiodes with the indicated Tb thicknesses.

The next rare earth element to be studied was Tb. Terbium layers were deposited onto the surfaces of six silicon photodiodes with thicknesses ranging from 7 nm to 170 nm. A protective capping layer of 7.6 nm Si was

deposited onto each Tb-coated photodiode without breaking vacuum. The measured transmittances of the Tb/Si bilayers on the six photodiodes are shown in Fig. 14. Terbium is relatively transmissive near 63 nm wavelength and is a potential candidate for high-reflectance multilayer coatings at this wavelength.

6. SUMMARY

The development of multilayer-coated gratings for solar spaceflight instruments has motivated the study of the optical constants of a number of elements. These include Y for the 9 nm wavelength region, Sc and Ti for 40-50 nm wavelengths, and La and Tb for >50 nm wavelengths. In general, it has been found that the CXRO tables, while generally accurate and quite useful for the shorter wavelengths <20 nm, are in many cases not sufficiently accurate for wavelengths >30 nm. This is primarily because of the difficulty of performing accurate measurements owing to oxidation, contamination, and molecular effects, particularly for reactive elements. Some reactive elements, including the rare earth elements, are potential candidates for multilayer coatings for >50 nm wavelengths, and a novel technique is being utilized for the determination of the optical constants of reactive elements. Layers are deposited onto the surfaces of silicon photodiodes and are protected by thin capping layers. A systematic study of the optical constants of reactive elements that are potentially transmissive in the >50 nm wavelength region is in progress.

REFERENCES

1. J. Seely, Proc. SPIE **4138**, 174 (2000).
2. C. Korendyke, C. Brown, J. Seely, and S. Meyers, OE Mag. **2**, 23 (2002).
3. D. Windt, S. Donguy, J. Seely, and B. Kjornrattanawanich, Appl. Opt. **43**, 1835 (2004).
4. J. Seely, C. Brown, D. Windt, S. Donguy, and B. Kjornrattanawanich, Appl. Opt. **43**, 1463 (2004).
5. B. Henke, E. Gullikson, and J. Davis, At. Data Nucl. Data Tables, **54**, 181 (1993). www-cxro.lbl.gov.
6. C. Tarrio, R. Watts, T. Lucatorto, J. Slaughter, and C. Falco, Appl. Opt. **37**, 4100 (1998).
7. L. Goray, International Intellectual Group Inc., P. O. Box 335, Penfield NY 14526, www.pcgrate.com.
8. L. Goray and J. Seely, Appl. Opt. **41**, 1434 (2002).
9. C. Montcalm, S. Bajt, and J. Seely, Opt. Lett. **26**, 125 (2001).
10. J. Seely, C. Montcalm, S. Baker, and S. Bajt, Appl. Opt. **40**, 5565 (2001).
11. J. Seely, L. Goray, W. Hunter, and J. Rife, Appl. Opt. **38**, 1251 (1999).
12. M. Kowalski, J. Seely, L. Goray, W. Hunter, and J. Rife, Appl. Opt. **36**, 8939 (1997).
13. E. Arakawa, T. Callcott, and Y. Chang, in *Handbook of Optical Constants of Solids II*, ed. by E. Palik (Academic Press, New York, 1991), p. 421.
14. D. Lynch and W. Hunter, in *Handbook of Optical Constants of Solids III*, ed. by E. Palik (Academic Press, New York, 1998), p. 253.
15. D. Lynch and W. Hunter, in *Handbook of Optical Constants of Solids*, ed. by E. Palik (Academic Press, New York, 1985), p. 303.
16. C. Montcalm, B. Sullivan, M. Ranger, and H. Pepin, J. Vac. Sci. Technol. A **15**, 3069 (1997).
17. B. Sae-Lao, S. Bajt, C. Montcalm, and J. Seely, Appl. Opt. **41**, 2394 (2002).
18. B. Kjornrattanawanich, R. Soufli, S. Bajt, D. Windt, and J. Seely, Proc. SPIE (these proceedings).
19. Y. Uspenskii, V. Levashov, A. Vinogradov, A. Fedorenko, V. Kondratenko, Y. Pershin, and E. Zubarev, Opt. Lett. **23**, 771 (1998).
20. J. Seely, Y. Uspenskii, Y. Pershin, V. Kondratenko, and A. Vinogradov, Appl. Opt. **41**, 1846 (2002).
21. Y. Uspenskii, J. Seely, N. Popov, A. Vinogradov, Y. Pershin, and V. Kondratenko, J. Opt. Soc. Am. A **21**, 298 (2004).
22. A. Vinogradov, Y. Pershin, E. Zubaryev, D. Voronov, O. Penkov, V. Kondratenko, Y. Uspenskii, I. Artioukov, and J. Seely, Proc. SPIE **4505**, 230 (2001).
23. D. Lynch and W. Hunter, in *Handbook of Optical Constants of Solids*, ed. by E. Palik (Academic Press, New York, 1985), p. 357.
24. J. Larruquert and R. Keski-Kuha, Appl. Opt. **41**, 5398 (2002).
25. J. Weaver, C. Kafka, D. Lynch, and E. Koch, *Optical Properties of Metals II*, Physik Daten Nr. 18-2 (1981).

*john.seely@nrl.navy.mil; phone 1 202 767 3529